Acta Crystallographica Section F
Structural Biology and Crystallization Communications
ISSN 1744-3091

Crystallization and preliminary X-ray diffraction analysis of various enzyme–substrate complexes of isopropylmalate dehydrogenase from *Thermus thermophilus*

Angelo Merli,[a]‡ Karuppasamy Manikandan,[b]‡§ Éva Gráczer,[c] Linda Schuldt,[b] Rajesh Kumar Singh,[d] Péter Závodszky,[c] Mária Vas[c] and Manfred S. Weiss[b]*¶

[a]Department of Biochemistry and Molecular Biology, University of Parma, Viale G. P. Usberti 23/A, 43100 Parma, Italy, [b]EMBL Hamburg Outstation, c/o DESY, Notkestrasse 85, D-22603 Hamburg, Germany, [c]Institute of Enzymology, Biological Research Center, Hungarian Academy of Sciences, H1518 Budapest, PO Box 7, Hungary, and [d]National Chemical Laboratory, Dr Homi Bhabha Road, Pune 411 008, India

‡ These authors should be regarded as joint first authors.
§ Present address: Leiden University Medical Center, Molecular Cell Biology, Electron Microscopy Section, PO Box 9600, 2300 RC Leiden, The Netherlands.
¶ Present address: Helmholtz-Zentrum Berlin für Materialien und Energie, Macromolecular Crystallography (BESSY-MX), Albert-Einstein-Strasse 15, D-12489 Berlin, Germany.

Correspondence e-mail: msweiss@helmholtz-berlin.de

Received 16 April 2010
Accepted 3 May 2010

The *Thermus thermophilus* 3-isopropylmalate dehydrogenase (*Tt*-IPMDH) enzyme catalyses the penultimate step of the leucine-biosynthesis pathway. It converts (2*R*,3*S*)-3-isopropylmalate to (2*S*)-2-isopropyl-3-oxosuccinate in the presence of divalent Mg^{2+} or Mn^{2+} and with the help of NAD^+. In order to elucidate the detailed structural and functional mode of the enzymatic reaction, crystals of *Tt*-IPMDH were grown in the presence of various combinations of substrate and/or cofactors. Here, the crystallization, data collection and preliminary crystallographic analyses of six such complexes are reported.

1. Introduction

The enzyme 3-isopropylmalate dehydrogenase (IPMDH, LeuB; EC 1.1.1.85) is part of the leucine-biosynthesis pathway (Hayashi-Iwasaki & Oshima, 2000) and catalyses the oxidative decarboxylation of β-3-isopropylmalate (IPM). The corresponding oxidant is NAD^+ and the reaction requires the presence of divalent Mg^{2+} or Mn^{2+}. Based on steady-state kinetic studies, a random mechanism of substrate binding has been proposed (Dean & Dvorak, 1995). However, the exact role of each substrate in inducing the catalytically competent conformation and the role of the metal ion in catalysis has not yet been clarified.

Three-dimensional structures of IPMDHs from various sources are known and exhibit great similarities. The biologically active enzyme is a dimer consisting of two identical subunits. Each subunit comprises two structural domains (Imada *et al.*, 1991, 1998; Hurley & Dean, 1994; Kadono *et al.*, 1995; Wallon *et al.*, 1997; Tsuchiya *et al.*, 1997; Singh *et al.*, 2005). The major interaction surface between the two subunits is formed by a characteristic arm consisting of two parallel β-strands linked by several salt bridges. This arm is especially pronounced in the enzyme from thermophilic sources (Németh *et al.*, 2000). Another interesting structural feature of the homodimeric enzyme is that the 3-isopropylmalate binding site in the active-site cleft of the enzyme is built up using amino-acid residues from both subunits.

A detailed comparison of the various IPMDH crystal structures revealed a significant domain motion between an open and a closed state of the enzyme (Singh *et al.*, 2005). This suggests that domain closure plays an essential role during the catalytic cycle, similar to the mechanism proposed for other multi-domain enzymes (Hayward, 2004; Gerstein & Echols, 2004). The most closed structure was obtained in crystals of IPMDH from *Thiobacillus ferrooxidans* (*Tf*-IPMDH) in complex with IPM (Imada *et al.*, 1998), although the substrate-free structure of *Mycobacterium tuberculosis* IPMDH (*Mtb*-IPMDH) also exhibits an almost completely closed conformation (Singh *et al.*, 2005). In addition, there is some evidence from small-angle X-ray scattering data that not only 3-isopropylmalate (IPM) but also NAD^+ is able to induce a partially closed state in *Thermus thermophilus* IPMDH (*Tt*-IPMDH; Kadono *et al.*, 1995). On the other hand, in the case of isocitrate dehydrogenase (ICDH), an

enzyme with a similar catalytic mechanism and with similar structural characteristics (Hurley *et al.*, 1991), only $NADP^+$ seems to be able to induce domain closure, while the substrate isocitrate is not. Thus, neither the exact molecular mechanism of the domain closure of IPMDH nor the role of each substrate and the metal ion has been clarified. In this context, it is notable that structures of the various IPMDH–substrate complexes have not yet been determined from the same species.

Therefore, we have undertaken the crystallization of *Tt*-IPMDH in various forms: the apoenzyme in both the absence and the presence of Mn^{2+}; the enzyme in complex with Mn^{2+} and the substrate IPM; in complex with Mn^{2+} and NAD^+; and in complex with Mn^{2+} and NADH; and the nonfunctioning quaternary complex of IPMDH with Mn^{2+}, IPM and NADH. In all crystallization experiments it was ensured that no anions that could interfere with the binding of the substrate were present. Here, we report the crystallization conditions and the preliminary characterization of these crystals by X-ray diffraction methods. The elucidation of the corresponding structures is currently under way with the aim of obtaining a detailed description of the molecular mechanism of substrate-induced conformational transitions as well as the structural background of the catalytic mechanism of IPMDH. Since IPMDH is an essential enzyme for bacteria but is absent in humans, structural information on the bacterial enzyme may also be of great relevance to structure-based drug-design efforts.

2. Experimental methods

2.1. Expression and purification

The *Tt*-IPMDH construct that was expressed contained the three additional amino acids MAS at its N-terminus and a linker and a hexa-His tag with the sequence AAALEHHHHHH at its C-terminus (Gráczer *et al.*, 2007). Briefly, protein expression was carried out in BL21 (DE3) pLysS *Escherichia coli* cells containing the pET21c plasmid (EMD Biosciences) carrying the appropriate *Tt*-IPMDH gene. The cells were grown at 310 K in the presence of 100 mg ml^{-1} ampicillin and 30 mg ml^{-1} chloramphenicol. Protein expression was induced with 0.4 m*M* isopropyl β-D-1-thiogalactopyranoside (IPTG). The enzyme was purified by Ni^{2+}–NTA affinity chromatography using

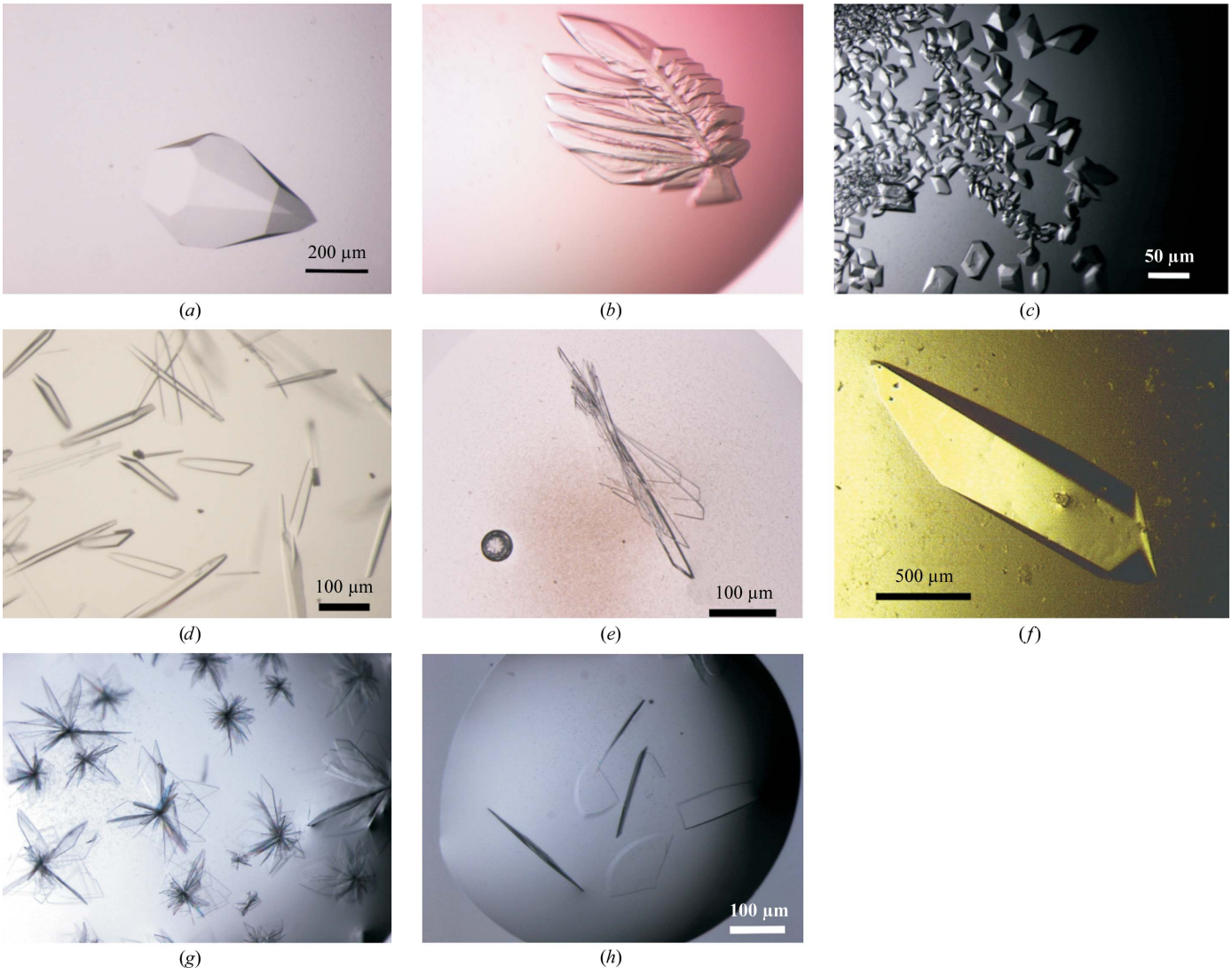

Figure 1
Crystals of *Tt*-IPMDH grown in the presence of various combinations of substrate and cofactors. (*a*) Apo *Tt*-IPMDH, (*b*, *c*) *Tt*-IPMDH grown in the presence of Mn^{2+} before (*b*) and after (*c*) streak-seeding, (*d*) tertiary complex of *Tt*-IPDMH with IPM and Mn^{2+}, (*e*) tertiary complex of *Tt*-IPMDH with NADH and Mn^{2+}, (*f*) tertiary complex of *Tt*-IPMDH with NAD^+ and Mn^{2+}, (*g*, *h*) quaternary complex of *Tt*-IPMDH with NADH, IPM and Mn^{2+} before (*g*) and after (*h*) streak-seeding.

Table 1
Data-collection and processing statistics.

Values in parentheses are for the highest resolution shell.

Protein–substrate complex	Apo *Tt*-IPMDH	*Tt*-IPMDH–Mn^{2+}	*Tt*-IPMDH–IPM–Mn^{2+}	*Tt*-IPMDH–NADH–Mn^{2+}	*Tt*-IPMDH–NADH–IPM–Mn^{2+}
Beamline	ID14-2, ESRF	X12, EMBL-HH DESY	X12, EMBL-HH DESY	ID23-2, ESRF	ID23-1, ESRF
No. of crystals	1	1	1	1	1
Wavelength (Å)	0.9334	1.000	1.000	0.873	0.9754
Crystal-to-detector distance (mm)	171	220	220	306.29	420.1
Rotation range per image (°)	0.5	0.5	0.5	1.0	0.3
Total rotation range (°)	125	180	200	200	180
Resolution range (Å)	99.0–1.83 (1.86–1.83)	99.0–2.50 (2.56–2.50)	99.0–2.20 (2.24–2.20)	99.0–2.50 (2.56–2.50)	99.0–2.75 (2.80–2.75)
Space group	$P3_221$	$P2_12_12$	$C222_1$	$P2_1$	$P2_12_12$
Unit-cell parameters (Å, °)	$a = b = 76.48$, $c = 154.30$	$a = 85.49$, $b = 112.0$, $c = 82.26$	$a = 50.24$, $b = 146.34$, $c = 175.21$	$a = 56.38$, $b = 161.45$, $c = 83.91$, $\beta = 91.96$	$a = 161.87$, $b = 175.0$, $c = 114.12$
Mosaicity (°)	0.84	0.62	0.80	0.50	0.7
Total No. of reflections	283997	189699	264018	217921	549812
Unique reflections	47324	27686	33360	51742	82490
Redundancy	6.0 (4.5)	6.9 (6.7)	7.9 (7.3)	4.2 (3.8)	6.7 (4.4)
Completeness (%)	99.0 (91.2)	98.7 (99.5)	99.9 (99.9)	99.9 (99.0)	97.2 (79.1)
$\langle I/\sigma(I)\rangle$	16.7 (2.4)	16.3 (2.0)	24.0 (4.6)	10.8 (2.1)	12.2 (2.2)
R_{merge} (%)	8.3 (64.6)	12.3 (94.0)	10.1 (55.4)	13.1 (57.1)	14.6 (54.3)
$R_{r.i.m.}$† (%)	9.0 (68.4)	16.6 (102.2)	10.8 (58.3)	15.0 (66.5)	15.8 (60.9)
$R_{p.i.m.}$† (%)	3.4 (30.8)	6.3 (38.9)	3.7 (20.8)	7.3 (33.3)	6.0 (27.0)
Overall *B* factor from Wilson plot ($Å^2$)	29.1	61.5	48.7	44.0	56.2
Optical resolution‡ (Å)	1.55	1.92	1.76	1.83	1.99
V_M ($Å^3$ Da^{-1})	3.62	2.59	2.12	2.51	2.66
Solvent content (%)	66	53	42	51	54
Estimated No. of molecules in the asymmetric unit	1	2	2	4	8

† Redundancy-independent merging *R* factor $R_{r.i.m} = 100\sum_{hkl}[N/(N-1)]^{1/2}\sum_i|I_i(hkl) - \langle I(hkl)\rangle|/\sum_{hkl}\sum_i I_i(hkl)$, where *N* is the number of times a given reflection *hkl* was observed; precision-indicating merging *R* factor $R_{p.i.m} = 100\sum_{hkl}[1/(N-1)]^{1/2}\sum_i|I_i(hkl) - \langle I(hkl)\rangle|/\sum_{hkl}\sum_i I_i(hkl)$ (Weiss, 2001). ‡ Defined as in Vaguine *et al.* (1999).

100 m*M* imidazole for elution in 50 m*M* sodium phosphate buffer pH 8.0 containing 300 m*M* NaCl. The collected protein fractions were dialyzed against the buffer 25 m*M* MOPS pH 7.6. The purity of the *Tt*-IPMDH was assessed by SDS–PAGE stained with Coomassie Brilliant Blue, where a single band was observed. The purified enzyme solution at a concentration of 15–20 mg ml^{-1} was frozen in liquid nitrogen, lyophilized and stored at 193 K.

2.2. Crystallization

The pure lyophilized *Tt*-IPMDH protein was dissolved in distilled water to a concentration of 24.5 mg ml^{-1} and the other compounds were added from concentrated stock solutions in water in order to achieve the reported final concentrations. The hanging-drop vapour-diffusion method was used with a typical drop size of 2 µl (1 µl protein solution and 1 µl reservoir solution) and 500 µl reservoir solution. All crystallization experiments were carried out at room temperature.

2.2.1. Apo *Tt*-IPMDH. Crystals of apo *Tt*-IPMDH were obtained by mixing the protein solution at a concentration of 18 mg ml^{-1} with reservoir solution consisting of 35–40%(*v*/*v*) PEG 550 MME, 0.1 *M* Tris–HCl pH 9.0 and 0.1 *M* NaCl. Bipyramidal crystals appeared in about a week (Fig. 1*a*).

2.2.2. *Tt*-IPMDH in complex with Mn^{2+}. Crystals of *Tt*-IPMDH in complex with Mn^{2+} ions were obtained by mixing 1 µl protein solution at a concentration of 11 mg ml^{-1} containing 22 m*M* $MnCl_2$ with 1 µl reservoir solution consisting of 5%(*w*/*v*) PEG 10 000 and 0.1 *M* HEPES pH 7.5. Initially, only highly intergrown crystals could be obtained (Fig. 1*b*). A microseed stock was prepared from these crystals by crushing some of them in 100 µl reservoir solution. A cat whisker was then used to streak-seed new drops which had been equilibrated for about 12 h. After 1 or 2 d, many single crystals appeared in the seeded drops (Fig. 1*c*).

2.2.3. *Tt*-IPMDH in complex with Mn^{2+} and IPM. Crystals of the ternary complex of *Tt*-IPMDH with Mn^{2+} and IPM were obtained by mixing protein solution consisting of 18 mg ml^{-1} *Tt*-IPMDH, 7 m*M* $MnCl_2$ and 7 m*M* IPM with reservoir solution consisting of 10%(*w*/*v*) PEG 4000, 10%(*v*/*v*) 2-propanol and 0.1 *M* HEPES pH 7.5. Long rectangular crystals appeared after one week (Fig. 1*d*).

2.2.4. *Tt*-IPMDH in complex with Mn^{2+} and NADH. Crystals of the ternary complex of *Tt*-IPMDH with Mn^{2+} and NADH were obtained by mixing 1 µl of a solution consisting of 18 mg ml^{-1} *Tt*-IPMDH, 7 m*M* $MnCl_2$ and 7 m*M* NADH with 1 µl reservoir solution consisting of 15%(*w*/*v*) PEG 20 000, 2%(*v*/*v*) dioxane and 0.1 *M* Bicine pH 9.0. A stack of long plate-shaped crystals appeared in about three weeks (Fig. 1*e*).

2.2.5. *Tt*-IPMDH in complex with Mn^{2+} and NAD^+. Crystals of the ternary complex of *Tt*-IPMDH with Mn^{2+} and NAD^+ were obtained by mixing 1 µl of a solution consisting of 20 mg ml^{-1} *Tt*-IPMDH, 2 m*M* $MnCl_2$ and 4.5 m*M* NAD^+ with 1 µl reservoir solution consisting of 13.5%(*w*/*v*) PEG 6000, 4.5%(*v*/*v*) MPD and 0.1 *M* HEPES pH 7.5. Long thick crystals appeared in about three weeks (Fig. 1*f*).

2.2.6. *Tt*-IPMDH in complex with Mn^{2+}, IPM and NADH. Crystals of the quaternary complex of *Tt*-IPMDH with Mn^{2+}, IPM and NADH were obtained by mixing protein solution consisting of 20 mg ml^{-1} *Tt*-IPMDH, 2 m*M* $MnCl_2$, 2 m*M* IPM and 4 m*M* NADH with reservoir solution consisting of 10%(*w*/*v*) PEG 10 000 and 0.1 *M* HEPES pH 7.5. After two weeks, thin stacked plate-like crystals appeared (Fig. 1*g*). Microseeds were prepared from these crystals as described for the binary complex crystals (see §2.2.2). New drops were then equilibrated for 1 d before being streak-seeded. Plate-like single crystals grew in the seeded drop after 2 d (Fig. 1*h*).

2.3. Diffraction data collection and processing

All diffraction experiments were carried out at 100 K in a nitrogen stream using a single suitably cryoprotected crystal. Indexing and integration of the data were performed using the program *DENZO* (Otwinowski & Minor, 1997), followed by scaling and merging using *SCALEPACK* (Otwinowski & Minor, 1997). The *R* factors $R_{r.i.m.}$

(redundancy-independent merging R factor) and $R_{\rm p.i.m.}$ (precision-indicating merging R factor) (Weiss, 2001) were calculated using the program *RMERGE* (available from http://www.embl-hamburg.de/~msweiss/projects/msw_qual.html or from MSW upon request). The data-collection parameters and processing statistics are summarized in Table 1. Intensities were converted to structure-factor amplitudes using the program *TRUNCATE* (French & Wilson, 1978; Collaborative Computational Project, Number 4, 1994). The optical resolution of the data sets was calculated with *SFCHECK* (Vaguine *et al.*, 1999) and the self-rotation functions were computed using the program *MOLREP* (Collaborative Computational Project, Number 4, 1994) based on structure-factor amplitudes to a maximum resolution of 4.0 Å. All data sets were also analyzed for twinning and pseudo-translational symmetry using *SFCHECK* (Vaguine *et al.*, 1999).

2.3.1. Apo *Tt*-IPMDH. A single crystal was mounted in a suitably sized nylon loop and cryoprotected using 0.1 *M* NaCl, 0.1 *M* Tris–HCl pH 9.0, 45%(*v*/*v*) PEG 550 MME and 10%(*v*/*v*) glycerol for 10–15 s. The crystal was then flash-cooled in liquid nitrogen. Data collection was carried out on the ESRF (Grenoble, France) beamline ID14-2 using an ADSC Quantum 4 CCD detector. The crystal diffracted to a resolution of about 1.8 Å.

2.3.2. *Tt*-IPMDH in complex with Mn^{2+}. Although the crystals were grown at room temperature, crystal mounting was carried out in

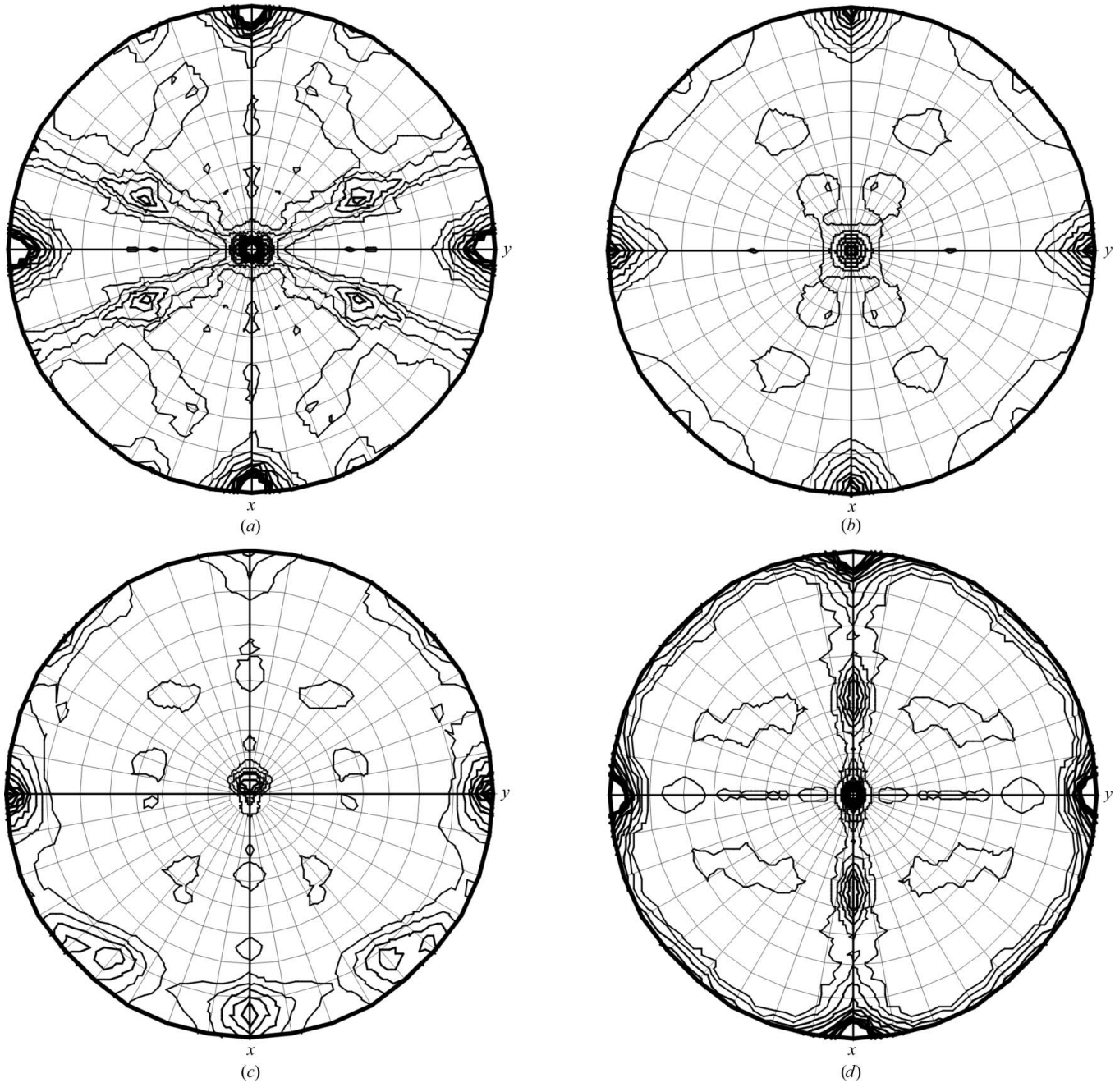

Figure 2
Self-rotation functions based on data collected from various *Tt*-IPMDH crystals. Shown are the $\kappa = 180^{\circ}$ sections of (*a*) the binary complex between *Tt*-IPMDH and Mn^{2+}, (*b*) the ternary complex of *Tt*-IPMDH with IPM and Mn^{2+}, (*c*) the ternary complex of *Tt*-IPMDH with NADH and Mn^{2+} and (*d*) the quaternary complex of *Tt*-IPMDH with NADH, IPM and Mn^{2+}. This figure was produced using the program *MOLREP* (Collaborative Computational Project, Number 4, 1994).

a cold room because the crystals frequently cracked when mounting was attempted at 293 K. A single crystal was harvested and soaked in cryobuffer consisting of 15%(*w*/*v*) PEG 10 000, 0.1 *M* HEPES pH 7.5 and 10%(*v*/*v*) glycerol. After 10–15 s, the crystal was flash-cooled in liquid nitrogen. Subsequently, diffraction data collection was carried out on EMBL beamline X12 (DESY Hamburg, Germany). Beamline X12 is equipped with a MARdtb and a MAR Mosaic 225 mm CCD detector. The crystal diffracted to a maximum resolution of 2.5 Å.

2.3.3. *Tt*-IPMDH in complex with Mn^{2+} and IPM. A single crystal was harvested with a nylon loop and soaked in cryoprotectant solution consisting of 10%(*v*/*v*) 2-propanol, 0.1 *M* HEPES pH 7.5, 25%(*w*/*v*) PEG 4000 and 15%(*v*/*v*) glycerol for 10–15 s before being directly flash-cooled in a nitrogen stream at the beamline. Diffraction data collection was carried out on EMBL beamline X12 (DESY Hamburg, Germany). The crystal diffracted to a maximum resolution of 2.2 Å.

2.3.4. *Tt*-IPMDH in complex with Mn^{2+} and NADH. A single crystal was harvested using a suitably sized nylon loop and soaked in cryoprotectant solution containing 2%(*v*/*v*) dioxane, 0.1 *M* Bicine pH 9.0 and 15%(*w*/*v*) PEG 20 000 supplemented with 10%(*v*/*v*) glycerol. After 10–15 s, it was flash-cooled in liquid nitrogen and stored. Diffraction data collection was carried out on beamline ID23-2 at the ESRF synchrotron (Grenoble, France). ID23-2 is equipped with a MAR Mosaic 225 mm CCD detector. The crystal diffracted to a maximum resolution of 2.5 Å.

2.3.5. *Tt*-IPMDH in complex with Mn^{2+}, IPM and NADH. A single crystal was harvested using a nylon loop and soaked for 10–15 s in a cryoprotectant solution consisting of 0.1 *M* HEPES pH 7.5, 10%(*w*/*v*) PEG 10 000 and 10%(*v*/*v*) glycerol. It was subsequently flash-cooled in liquid nitrogen and stored until transport to the beamline. Diffraction data collection was carried out on beamline ID23-1 at the ESRF synchrotron (Grenoble, France). ID23-1 is equipped with an ADSC Q315r CCD detector. The diffraction limit of the crystal was observed to be about 2.75 Å.

3. Results and discussion

3.1. Data collection and analysis of the diffraction data

The data-collection parameters and the final statistics of the processed data are summarized in Table 1 for the crystals described above. Complete and high-quality diffraction data could be collected for all of the crystals apart from those of the ternary complex of *Tt*-IPMDH with Mn^{2+} and NAD^+. Pseudo-translational symmetry appears to be present in one of the data sets (see §3.1.5), but no twinning was observed in any of the data sets.

3.1.1. Apo *Tt*-IPMDH. The bipyramidal crystal of the apoenzyme was significantly thicker than any of the other analyzed crystals. Consequently, the resolution of the data obtained was the highest, at about 1.8 Å. Interestingly, despite the fact that the apoenzyme crystal belonged to the same trigonal space group $P3_221$ (Table 1) and exhibited very similar unit-cell parameters as the previously reported crystals (Katsube *et al.*, 1988; Sakurai *et al.*, 1992; Nagata *et al.*, 1996; Tsuchiya *et al.*, 1997), the crystallization conditions were different. While the crystals reported here were grown at high pH from PEG 550 MME, the previous crystals were all grown at near-physiological pH from high concentrations of phosphate and/or sulfate.

3.1.2. *Tt*-IPMDH in complex with Mn^{2+}. The crystal of the binary complex diffracted X-rays to about 2.5 Å resolution. Owing to an ice ring in the diffraction pattern, the completeness values in the 3.88–3.61 Å and 3.61–3.39 Å resolution bins were only 86.6% and 96.1%, respectively, despite the quite satisfactory overall completeness of 98.7% (Table 1). The ice ring also led to an artificial peak in the Wilson plot. The content of the asymmetric unit of the orthorhombic crystals of space group $P2_12_12$ is most probably a *Tt*-IPMDH homodimer. This corresponds to a Matthews parameter V_M of 2.59 $Å^3\ Da^{-1}$ and a solvent content of 53% (Matthews, 1968) and is supported by a clear peak at ($\theta = 52^\circ$, $\varphi = 65^\circ$) in the $\kappa = 180^\circ$ section of the self-rotation function (Fig. 2*a*).

3.1.3. *Tt*-IPMDH in complex with Mn^{2+} and IPM. The *Tt*-IPMDH crystal grown in the presence of IPM and Mn^{2+} diffracted X-rays to a maximum resolution of 2.2 Å (Table 1). Despite the rather high $I/\sigma(I)$ value of 4.6 in the outer resolution bin (Table 1), the data were cut at this resolution because of Wilson plot anomalies beyond 2.2 Å. The crystal belonged to the *C*-centred orthorhombic space group $C222_1$. The most likely content of the asymmetric unit is one *Tt*-IPMDH dimer. For two molecules in the asymmetric unit, the Matthews coefficient (Matthews, 1968) would be 2.12 $Å^3\ Da^{-1}$, with a corresponding solvent content of 42%. Nevertheless, no clear peak could be observed in the $\kappa = 180^\circ$ section of the self-rotation function (Fig. 2*b*).

3.1.4. *Tt*-IPMDH in complex with Mn^{2+} and NADH. A complete 2.5 Å data set was collected from the crystal grown in the presence of the cofactor NADH and Mn^{2+} (Table 1). The crystal belonged to the primitive monoclinic space group $P2_1$. Assuming the presence of two dimers in the asymmetric unit, V_M is 2.51 $Å^3\ Da^{-1}$ and the solvent content is 51%. This notion is supported by the presence of two peaks in the $\kappa = 180^\circ$ section of the self-rotation function (Fig. 2*c*). One of the peaks is close to the *z* axis and the other is close to the *x* axis of the crystal, which together with the crystallographic peak along *y* would support a 222 symmetric arrangement of the *Tt*-IPMDH molecules in the asymmetric unit.

3.1.5. *Tt*-IPMDH in complex with Mn^{2+}, IPM and NADH. The crystal of the nonproductive quaternary complex of *Tt*-IPMDH with Mn^{2+}, IPM and NADH diffracted X-rays to a maximum resolution of about 2.75 Å. In order to avoid overlapping reflections an oscillation width of 0.3° per image had to be used. The total crystal rotation was 180° and all collected images were used for processing and scaling. Nevertheless, the final processed data showed only 79% completeness in the high-resolution bin (2.81–2.75 Å) and 97% completeness overall. The crystal belonged to the primitive orthorhombic space group $P2_12_12$. The most likely number of *Tt*-IPMDH molecules in the asymmetric unit is eight (four *Tt*-IPMDH homodimers). The corresponding value of V_M is 2.66 $Å^3\ Da^{-1}$ and the solvent content is 54%. The self-rotation function (Fig. 2*d*) remains inconclusive with regard to the number of molecules, since only one clear noncrystallographic peak can be observed between the *x* and *z* axes of the crystal. Two non-origin peaks were observed at (0.00, 0.02, 0.50) and (0.05, 0.50, 0.44), indicating the presence of pseudo-translational symmetry.

In previous crystallographic studies of IPMDH, crystals were mainly grown in the presence of high concentrations of sulfate or phosphate (Katsube *et al.*, 1988; Imada *et al.*, 1991; Nagata *et al.*, 1996; Wallon *et al.*, 1997; Tsuchiya *et al.*, 1997; Singh *et al.*, 2005). Only a few examples of IPMDH crystals grown from PEG have been reported to date (Wallon *et al.*, 1997; Tsuchiya *et al.*, 1997). Binary complexes with NAD^+ or with the analogue ADP-ribose were also crystallized in the presence of a high concentration of sodium formate (Hurley & Dean, 1994; Kadono *et al.*, 1995). Only the crystals of the ternary complex with IPM and Mg^{2+} (Imada *et al.*, 1998) as well as the quaternary complex with IPM, Mg^{2+} and a substrate-analogue inhibitor (Nango *et al.*, 2009) were obtained and/or stabilized in the presence of high concentrations of PEG. However, even in these latter cases $MgSO_4$ was present at concentrations of 40 m*M* (Imada *et al.*, 1998) and 1 m*M* (Nango *et al.*, 2009), respectively. In the present work, we have

tried to avoid the use of certain salts at high concentrations in order to prevent their possible interference with the binding of the anionic substrate.

Determination of all structures is currently in progress.

4. Summary

Successful crystallization of *Tt*-IPMDH in six different complexed forms has been reported and data have successfully been collected from five of these six crystals. The corresponding refined crystal structures will most likely represent various snapshots of structural intermediates along the enzymatic reaction coordinate. A comprehensive structural analysis of these different substrate-bound and/or cofactor-bound complexes is expected to provide detailed information on the role of each molecule in causing the conformational changes that are necessary for catalysis.

We would like to acknowledge the support of this work by various funding organizations: KM was supported by a postdoctoral research fellowship from the Alexander-von-Humboldt foundation, MV and ÉG by grant OTKA NK 77978 from the Hungarian National Research Fund, and AM by grant PRIN 20074TJ3ZB_004 from the Ministry of University and Research (MIUR). We would also like to thank the ESRF (Grenoble, France) and EMBL-HH (DESY Hamburg, Germany) for the allocation and provision of synchrotron beam time.

References

Collaborative Computational Project, Number 4 (1994). *Acta Cryst.* D**50**, 760–763.
Dean, A. M. & Dvorak, L. (1995). *Protein Sci.* **4**, 2156–2167.
French, S. & Wilson, K. (1978). *Acta Cryst.* A**34**, 517–525.
Gerstein, M. & Echols, N. (2004). *Curr. Opin. Chem. Biol.* **8**, 14–19.
Gráczer, É., Varga, A., Hajdú, I., Melnik, B., Szilágyi, A., Semisotnov, G., Závodszky, P. & Vas, M. (2007). *Biochemistry*, **46**, 11536–11549.
Hayashi-Iwasaki, Y. & Oshima, T. (2000). *Methods Enzymol.* **324**, 301–322.
Hayward, S. (2004). *J. Mol. Biol.* **339**, 1001–1021.
Hurley, J. H. & Dean, A. M. (1994). *Structure*, **2**, 1007–1016.
Hurley, J. H., Dean, A. M., Koshland, D. E. Jr & Stroud, R. M. (1991). *Biochemistry*, **30**, 8671–8678.
Imada, K., Inagaki, K., Matsunami, H., Kawaguchi, H., Tanaka, H., Tanaka, N. & Namba, K. (1998). *Structure*, **6**, 971–982.
Imada, K., Sato, M., Tanaka, N., Katsube, Y., Matsuura, Y. & Oshima, T. (1991). *J. Mol. Biol.* **222**, 725–738.
Kadono, S., Sakurai, M., Moriyama, H., Sato, M., Hayashi, Y., Oshima, T. & Tanaka, N. (1995). *J. Biochem (Tokyo)*, **118**, 745–752.
Katsube, Y., Tanaka, N., Takenaka, A., Yamada, T. & Oshima, T. (1988). *J. Biochem.* **104**, 679-680.
Matthews, B. W. (1968). *J. Mol. Biol.* **33**, 491–497.
Nagata, C., Moriyama, H., Tanaka, N., Nakasako, M., Yamamoto, M., Ueki, T. & Oshima, T. (1996). *Acta Cryst.* D**52**, 623–630.
Nango, E., Yamamoto, T., Kumasaka, T. & Eguchi, T. (2009). *Bioorg. Med. Chem.* **17**, 7789–7794.
Németh, A., Svingor, A., Pocsik, M., Dobó, J., Magyar, C., Szilágyi, A., Gál, P. & Závodszky, P. (2000). *FEBS Lett.* **468**, 48–52.
Otwinowski, Z. & Minor, W. (1997). *Methods Enzymol.* **276**, 307–326.
Sakurai, M., Onodera, K., Moriyama, H., Matsumoto, O., Tanaka, N., Numata, K., Imada, K., Sato, M., Katsube, Y. & Oshima, T. (1992). *J. Biochem.* **112**, 173–174.
Singh, R. K., Kefala, G., Janowski, R., Mueller-Dieckmann, C., von Kries, J. P. & Weiss, M. S. (2005). *J. Mol. Biol.* **346**, 1–11.
Tsuchiya, D., Sekiguchi, T. & Takenaka, A. (1997). *J. Biochem. (Tokyo)*, **122**, 1092–1104.
Vaguine, A. A., Richelle, J. & Wodak, S. J. (1999). *Acta Cryst.* D**55**, 191–205.
Wallon, G., Kryger, G., Lovett, S. T., Oshima, T., Ringe, D. & Petsko, G. A. (1997). *J. Mol. Biol.* **266**, 1016–1031.
Weiss, M. S. (2001). *J. Appl. Cryst.* **34**, 130–135.